Analytical Methods

In-situ and Real Time Investigation of Foliarly Applied Silver Nanoparticles on and in Spinach Leaves by Surface Enhanced Raman Spectroscopic Mapping

Journal:	*Analytical Methods*
Manuscript ID	AY-ART-03-2021-000346.R1
Article Type:	Paper
Date Submitted by the Author:	04-May-2021
Complete List of Authors:	Zhang, Zhiyun; University of Massachusetts, Amherst, Food Science Shang, Heping; University of Massachusetts, Amherst, Xing, Baoshan; UMASS, Stockbridge School of Agriculture He, Lili; Univ. of Massachusetts, Dept. of Food Science

In-situ and Real Time Investigation of Foliarly Applied Silver Nanoparticles on and in Spinach Leaves by Surface Enhanced Raman Spectroscopic Mapping

Zhiyun Zhang[1], Heping Shang[2], Baoshan Xing[2], and Lili He[1]

[1]Department of Food Science, University of Massachusetts, Amherst, Massachusetts 01003, United States

[2]Stockbridge School of Agriculture, University of Massachusetts, Amherst, Massachusetts 01003, United States

*** Corresponding Author:** Lili He,

Mailing Address: 240 Chenoweth Laboratory, 102 Holdsworth Way, Amherst, MA 01003,

E-mail: lilihe@foodsci.umass.edu,

Telephone: +1 (413) 545-5847

ABSTRACT

Understanding the behavior and biological fate of silver nanoparticles (AgNPs) applied on plant surfaces is significant for their risk assessment. Our study's objective is to investigate the interactions between AgNPs and plant biomolecules as well as to monitor and quantify the penetration of AgNPs in spinach by an *in-situ* and real-time surface enhanced Raman spectroscopic (SERS) mapping technique. AgNPs (2 μg per leaf) of different surface coating (citrate, CIT, and polyvinylpyrrolidone, PVP) and size (40 and 100 nm) were foliarly applied onto spinach leaves with different exposure time (1-48 h). Cysteine is the major biomolecule that interacts with AgNPs in spinach based on the *in-situ* and *in-vitro* SERS pattern recognition. The interaction between CIT-AgNPs and cysteine happened as soon as 1 h after AgNPs foliar deposition, which is faster than the interaction between PVP-AgNPs and cysteine. Also, the SERS depth mapping shows that particle size rather than surface coating determines the penetration capability of AgNPs in spinach, in which 40 nm AgNPs shows a deeper penetration than that of 100 nm. Last but not least, based on the results of SERS mapping, we detected significantly higher amounts of 40 nm CIT-/PVP-AgNPs than 100 nm CIT-AgNPs internalized in the leaf tissues after 1-hour exposure. The estimated percentage of internalized AgNPs (0.2-0.8%) was significantly smaller than that of the total residual Ag (9-12%), indicating the potential transformation of the AgNPs to other Ag species inside the plant tissues. This study facilitates a better understanding of the behaviors and biological fate of AgNPs in plant tissues.

1. INTRODUCTION

Colloidal silver has been known for their unique antimicrobial and insecticidal properties for over 120 years.[1] Researchers demonstrated the great potential of silver nanoparticles (AgNPs) to control insects[2-4] on crops and to avoid insecticide resistance.[2] In addition to be used as a pesticide, AgNPs have also been widely used in other commercialized products, including food production/packaging, biomedicine, personal care, cosmetics, textiles and so on.[3,4] According to the latest Nanotechnology Consumer Products Inventory, there are 442 out of a total 1827 listed Nano-based products that contain silver.[5] It is estimated that the global consumption of AgNPs will approximately reach 360 to 450 ton/year by the end of 2025.[6] With this growing production of AgNPs worldwide, however, concerns arise regarding the bioaccumulated AgNPs in crop plants that may cause harm to human beings. [2, 9-10] Therefore, investigation of the behaviors and biological fate of AgNPs in crops are essential for their safe and effective applications.

Up to now, the uptake of AgNPs in different plants has been extensively studied, although most of the studies have been focused on uptake through roots than leaves.[7–9] Among those studies that focused on foliar application, Larue et al. firstly observed that foliarly applied AgNPs can be entrapped by the cuticle and further penetrate into the leaf tissue through stomata by synchrotron radiation-based μXRF.[10] Through analyzing the speciation by Ag L_{III}-edge μXANES, they also found the oxidation of AgNPs and characterized the interactions between thiol-containing molecules and Ag^{+}/AgNPs. Following Larue's work, Li et al. studied the accumulation and phytotoxicity of AgNPs in soybean and rice.[10] With the help of sp-ICP-MS, they showed that the amounts of AgNPs that bioaccumulated in plants after foliar exposure are 17-200 times more than root exposure. In addition, they observed that foliarly applied AgNPs are mainly stored in the cell wall and plamalemma of leaves by TEM. Although these studies partially disclosure the underlying mechanism of how foliarly applied AgNPs penetrate into crop plants, no researchers have investigated the process of the AgNPs penetration in real time and quantified the amount of foliar penetration. These two knowledge gaps are mainly due to the lack of effective techniques and methods to monitor the penetration process in real time as well as to effectively remove the surface attached AgNPs and recover the internal AgNPs for quantifications.

We and others have demonstrated the capability of surface enhanced Raman spectroscopic (SERS) mapping to monitor the gold nanoparticles in plant tissues and characterize their interactions with plant bio-compounds.[11–13] SERS is an ultrasensitive vibrational spectroscopic technique that can provide rich information about the biocompounds that are in the vicinity of gold nanoparticles. Coupled with advanced mapping technique, researchers could collect thousands of spectra for every pixel within a defined sample area and constructed a colorimetric image based on the characteristic peaks of interested analytes. Thus, SERS mapping technique makes in-situ monitoring the localization of AuNPs in plant tissues possible. In addition, we developed an effective method to remove surface attached AgNPs on spinach and recovered around 50% of internal AgNPs by a newly developed organic solvent-based extraction method.[6] Through pre-concentrating those extracted AgNPs on a filter membrane and further quantifying their amounts by SERS mapping, we successfully lowered the lowest detectable concentration of AgNPs to 1 ng/mL.[14] Compared with sp-ICP-MS, which requires complex and tedious sample preparations, it only takes 15 min for one filter membrane scanning.

Based on these studies, we aimed to investigate the penetration process of foliarly applied AgNPs in plant leaves as well as *in-situ* characterize the interactions between AgNPs and biomolecules by SERS mapping technique. In addition, we quantitatively analyzed the amount of penetrated AgNPs after foliar penetration using the developed methods to remove surface attached AgNPs and recover penetrated AgNPs.[14] Two surface coatings, CIT- and PVP, and two sizes, 40 and 100 nm AgNPs were selected for this study.[15] Spinach was chosen because of its large global consumption and high edible tissue surface area, making it an ideal model to study the foliar transfer of NP contaminants.[6,16] To the best of our knowledge, this is the first study that provides real time data on the penetration process and quantitative analysis of AgNPs penetration, which will facilitate the risk assessment of the AgNPs for plant application and aid the development of safe and effective AgNPs-based pesticide products.

2. MATERIALS AND METHODS

2.1 Materials. Organic spinach leaves were purchased from Whole Foods Market (Amherst, MA) and transferred to the Chenoweth Lab at the University of Massachusetts Amherst. All spinach leaves were stored at 4 °C and used within 1 day. All leaves were washed with deionized water (Barnstead MicroPure system, Fisher Scientific Co., PA) with a pH of 5.85. AgNPs with different sizes (40 and 100 nm) and surface coating (citrate and polyvinylpyrrolidone) were purchased from Nanocomposix (San Diego, CA). According to the information given by the Nanocomposix (Figure S1), TEM shows that the sizes of 40 nm CIT-AgNPs, 40 nm PVP-AgNPs, and 100 nm CIT-AgNPs are 39 ± 4, 50 ± 4, and 97 ± 11, respectively. Also, the surface coatings of these commercial AgNPs were verified by comparing their SERS spectra with published references.[17] Both L-cysteine (Cys) and glutathione were acquired from Sigma-Aldrich (St. Louis, MO).

2.2 *In-situ* Characterize Foliarly Applied AgNPs and Their Penetration in Spinach. Ten droplets of 10 μL aliquot of the 20 mg/L AgNPs solution with different sizes (40 and 100 nm) and surface coating (citrate and polyvinylpyrrolidone) was dropwise added onto the spinach leaf surface. After AgNPs treated spinach leaves were air-dried at room temperature, SERS depth mapping images were acquired using a confocal DXR Raman microscope (Thermo Fisher Scientific, Madison, WI) with 50 μm pinhole aperture and 1 mW laser power. Each scanning area was randomly picked up from the AgNPs deposition on spinach leaf and vertical to leaf surface with 100 μm (length) × 300 (height) μm. The step size of the mapping along the Z-axis was 10 μm. The penetration behavior of AgNPs in spinach was monitored at different exposure time (1, 6, 12, 24 and 48 h).

2.3 Determination of the SERS Characteristic Signals of Biomolecules. Based on the *in-situ* characteristic peaks of AgNPs, we proposed the biomolecules that interact with AgNPs in spinach contain thiol groups, which may be L-Cysteine and glutathione. Thus, L-Cysteine and glutathione (0.01 g) powder were dissolved in 10 mL deionized water (DI water) and were further diluted to 100 mg/L, respectively. After that, 50 μL aliquot of each kind of AgNPs solution with 20 mg/L was added into them and mixed by a Fisher ScientificTM Analog vortex mixer (Fisher Scientific Co., PA) for 30 s, then 5 μL aliquot of mixture was transferred onto a piece of gold-coated microscope slide, and then allowed to dry at room temperature. SERS spectra were collected with a 50 μm slit aperture and 5 mW laser power to maximize the signals. Eight discrete locations were randomly chosen on each sample for analysis.

2.4 Quantification of Penetrated AgNPs in Spinach. To quantify internalized AgNPs, those surface attached AgNPs on spinach were removed by a combined sodium hypochlorite and ammonium hydroxide washing method.[6] Briefly, a piece of intact AgNPs-contaminated (2 μg) spinach leaves was sequentially immersed in Clorox bleach (200 mg/L, 50 mL, 5 min) and ammonium hydroxide solution ($NH_3 \cdot H_2O$, 50 mL, 1 min), with a final rinse by deionized water (DI Water, 50 mL, 1 min).

After washing, we immersed spinach leaves in a mixed acetone/methanol (V: V=4:1) solution that contains 1000 μg/mL 4-mercaptobenzoic acid (4-MBA). Two hours later, DI water and ethyl acetate were added into the methanol/acetone solution at an equal volume ratio and the pH of the resulting solution was adjusted using sodium hydroxide (wt 40%) to ≥9.0. All the surface attached 4-MBA molecules (pKa (carboxylic head group) ~7.4) were fully deprotonated after pH adjustment, which rendered those 4-MBA labelled AgNPs hydrophilic and forced them into the bottom layer of the solution. The extracted AgNPs were then enriched on a PTFE filter paper and analyzed on a Raman imaging microscope (DXRxi, Thermo Scientific, Waltham, MA) equipped with a 780 nm laser. The analysis was performed using a 20× confocal microscope objective, and 5 mW laser power. The slit aperture and acquisition time were set at 50 μm and 0.01 s, respectively. The data was collected and analyzed by OMNICxi and OMNIC 9.7 software (Thermo Scientific). The mapping image was constructed based on the characteristic peak height of 4-MBA at 1078 cm^{-1}. In this study, we set 1000 cps as the cut-off intensity to determine the presence of AgNPs on the SERS map, where the presence and the absence of AgNPs were marked as red and blue, respectively. The amounts of AgNPs were quantified through counting the percentage of pixel areas of the red spots in SERS image by ImageJ.

2.5 Inductively Coupled Plasma-Mass Spectrometry (ICP-MS). To determine the total amount of Ag elements in spinach leaves, spinach leaves with washing treatment were stored at ambient temperature prior to digestion. For the digestion process, spinach leaves were immersed with 3 mL HNO_3 (ACS reagent, 70%) in a 15 mL centrifuge tube overnight. Spinach leaves were heated to reach a temperature of 115 ℃ for 40 min, and then samples were cooled to room temperature. Five hundred μL of H_2O_2 was added to further digest the sample for 30 min. DI water was used to dilute the resultant digests to a total volume of 40

mL and then the diluent was filtered through polyethersulfone (PES) membrane prior to ICP-MS (Agilent 7500ce, Santa Clara, CA) analysis.

3. RESULTS AND DISCUSSION

3.1 *In-situ* Characterization of AgNPs in Spinach. To investigate the interactions between AgNPs and biomolecules in spinach as well as to understand their potential variations, the spectra of 40 nm CIT-AgNPs from three randomly selected positions were collected. As shown in Figure 1a, the spectra collected from different locations showed slightly different patterns. The highest peaks in these spectra are 685, 659 and 657 cm^{-1}, respectively. Although the positions of their highest peaks are slightly different, all these peaks could be assigned to C-S stretching. The Raman shift of the highest peaks may originate from different localized conditions, such as desorption, re-orientation, chemical transformation of the biomolecules on AgNPs surface. However, it should be noted that the pattern of SERS spectra collected from one position at different depth are similar. The SERS intensity gradually decreased with the depth increasing, which may result from the fact that less AgNPs are present in the deeper area (Figure 1b). It is noteworthy to mention that different enhanced biomolecule signals from AgNPs and AuNPs were observed, indicating different NPs-biomolecules interactions in spinach leaves. In our previous studies, we found AuNPs mainly interact with chlorophylls and carotenoids in spinach leaves.[11] We suppose this difference mainly comes from the different properties of AgNPs and AuNPs. For AuNPs, they are generally considered as more biologically inert than AgNPs and thus are commonly used in genetic engineering for DNA delivery to cells.[18–20] In contrast to AuNPs, AgNPs and the dissolved Ag^+ released from AgNPs are usually considered to be much more phytotoxic and may intrigue the production of detoxification biomolecules.[10,21,22] Thiol-containing ligands including cysteine, phytochelatins and metallothionein are supposed by Cobbett et al. to work as chelating agents to minimize the toxicity from AgNPs and the dissolved Ag^+.[23]

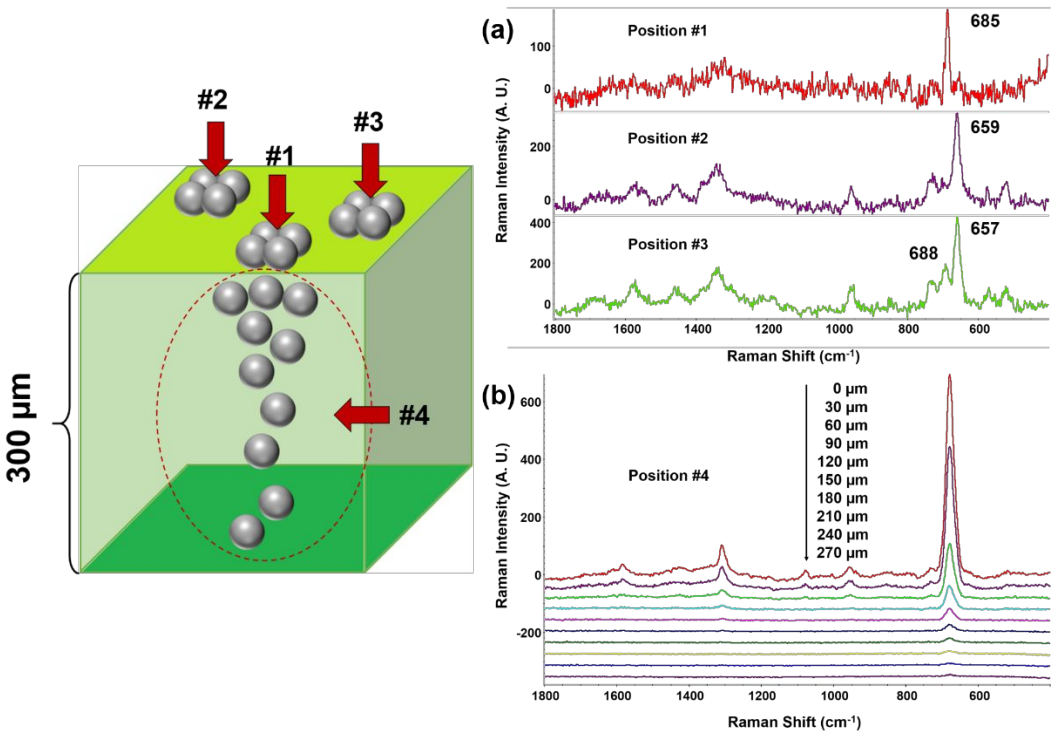

Figure 1. (a) SERS spectra of 40 nm CIT-AgNPs in different position of spinach leaf; (b) SERS spectra of 40 nm CIT-AgNPs in different depth (depth: 0 to 270 µm) of spinach leaf.

To further validate the SERS spectra were originated from the interaction between AgNPs and sulfur containing biomolecules, we collected the *in-vitro* SERS spectrum of AgNPs with cysteine (Cys) and glutathione (GSH). In addition to these two biomolecules, we also collected the SERS spectrum of chlorophyll since the interaction between AuNPs and chlorophyll had been reported in our previous study.[11] The SERS spectra of AgNPs (40 and 100 nm CIT, 40 nm PVP) and these biomolecules on a gold-coated slide were showed in Figure S2. Through comparison, we found the *in-vitro* SERS spectrum of AgNPs-cysteine is similar to the *in-situ* SERS spectrum of AgNPs, which exhibits enhanced SERS peaks in the 500-1700 cm^{-1} range, especially at 735, 664, 517 cm^{-1} (Figure 2). The peak at 517 cm^{-1} is assigned to the S-S stretching vibration, which could be considered as the characteristic of the disulphide band. According to the study given by Diaz Fleming et al., the appearance of the S-S stratching vibration suggests that two L-cysteine molecules come into being one L-cyteine through forming S-S bond.[24] In addition, two peaks, 735 and 664 cm^{-1}, are assigned to the C-S stretching vibration. Jing et al. mentioned that the peak at 735 cm^{-1} might be related to both P_N and P_C conformations,

indicating the L-cysteine molecules attach to the AgNPs via the carboxylate and amino groups.[25] Among these SERS peaks, the highest enhanced peak at 664 cm^{-1}, which comes from C-S stretching and is used as the characteristic peak to monitor the presence of AgNPs in spinach.

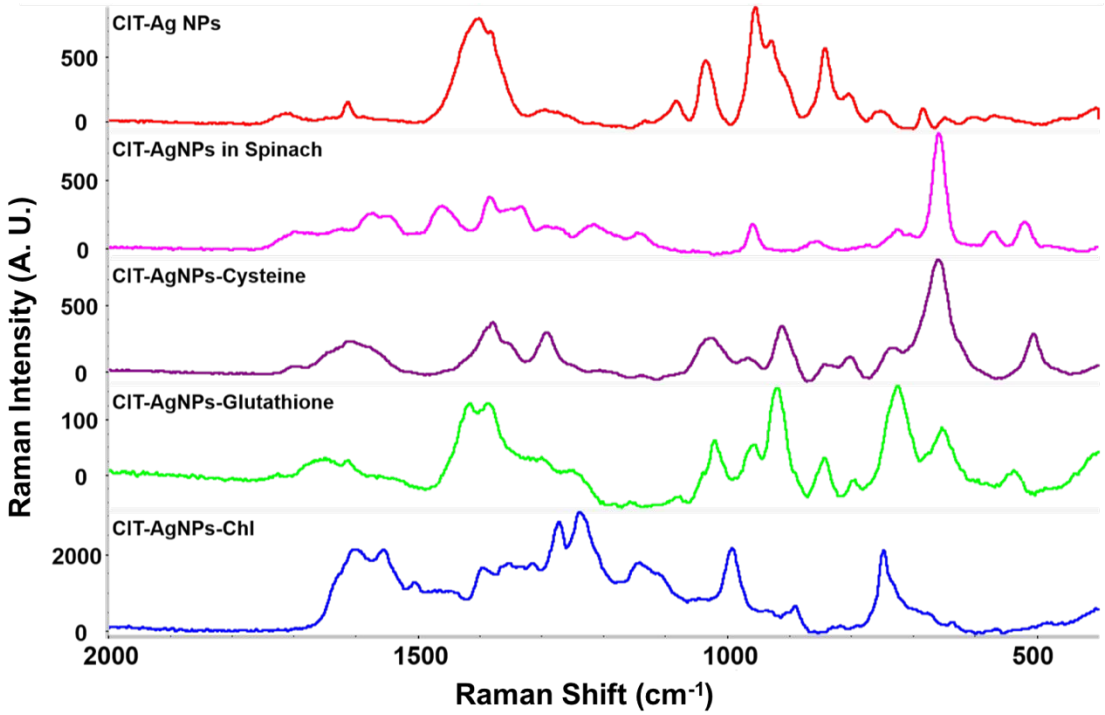

Figure 2. *in-vitro* SERS spectrum of AgNPs-cysteine and *in-situ* SERS spectrum of AgNPs in spinach.

3.2 Factors that Determine AgNPs' interaction and Penetration Behavior. According to previous studies, the penetration of AgNPs into plants is a complex process, depending on many factors (e.g. NP size, surface functionality, chemical composition).[26] Here, we first compared the penetration capability of AgNPs with different sizes (40 and 100 nm) in spinach. Figure 3a shows the *in situ* SERS spectrum of 40 nm CIT-AgNPs in spinach after different exposure time from 1 to 48 h. Compared with the spectrum of raw spinach and 40 nm CIT-AgNPs, characteristic peaks of cysteine at position 1033, 955, 735, 662 cm^{-1} can be observed after only 1 hour foliar exposure. This result indicates a rapid *in-situ* interaction between 40 nm CIT-AgNPs and cysteine in spinach. In addition to cysteine peaks, other SERS peaks could be observed in SERS spectra, which might originate from

other bio-components that are present in spinach, including pectin, lignin, or other polysaccharides.[27] Figure 3b shows the *in-situ* SERS spectrum of 100 nm CIT-AgNPs in spinach after same exposure time. Similar to 40 nm CIT-AgNPs, the characteristic peaks of cysteine, especially at 680-650 cm^{-1}, could also be observed after 1 h. It is noteworthy to mention that the intensity of C-S peak from cysteine became stronger with time increasing. We supposed that this is because of the increasing amounts of cysteine produced by plants in response to AgNPs. Ma et al. showed that the exposure of engineered *Crambe abyssinica* plants that express the bacterial γ-ECS to AgNPs resulted in a greater cysteine production.[21] Similar result was also reported by Li et al., the overexpression of γ-ECS in *Arabidopsis* contributes to a significant increase in cysteine upon arsenic treatment.[28]

From Figure 4a and 4d, the penetration depth of 40 nm CIT-AgNPs could reach to 183 ± 38 μm after 48 h. Compared with 40 nm CIT-AgNPs, we found that 100 nm CIT-AgNPs were mostly present closer to the spinach surface (90 ± 36 μm) even after 48 h, indicating the penetration cability of AgNPs is size dependent, which is consistent with other studies. For example, Eichert et al. observed the penetration of 43 nm fluorescent polystyrene NPs into plant leaves by confocal laser scanning microscopy whereas no uptake of 1.1 μm particles was observed.[29] Wang et al. investigated the penetration profile of four metal oxide NPs with size range from 24-47 nm in watermelon leaves.[30] They found small NPs could penetrate through the stomatal pathway into the watermelon leaves, and the metal elements were detected in both shoots and roots. In our previous study, we also found foilarly applied 50 nm AuNPs penetrate much deeper in the spinach leaves than 80 nm and 125 nm AuNPs.[11]

It should be noted that some authors found that the values of refractive index in fresh leaves ranged from 1.41 to 1.55, which might influence the depth resolution (equation 1). The influence will be further investigated in our future study.

$$\mathrm{DR} = \Delta\left\{\left[\frac{NA^2(n^2-1)}{1-NA^2} + n^2\right]^{1/2} - n\right\} \cdots\cdots (1)$$

Where DR is depth resolution, NA is the numerical aperture of the microscope objective, n (1.41~1.55) is the refractive index, and Δ is the attempted position of focus.

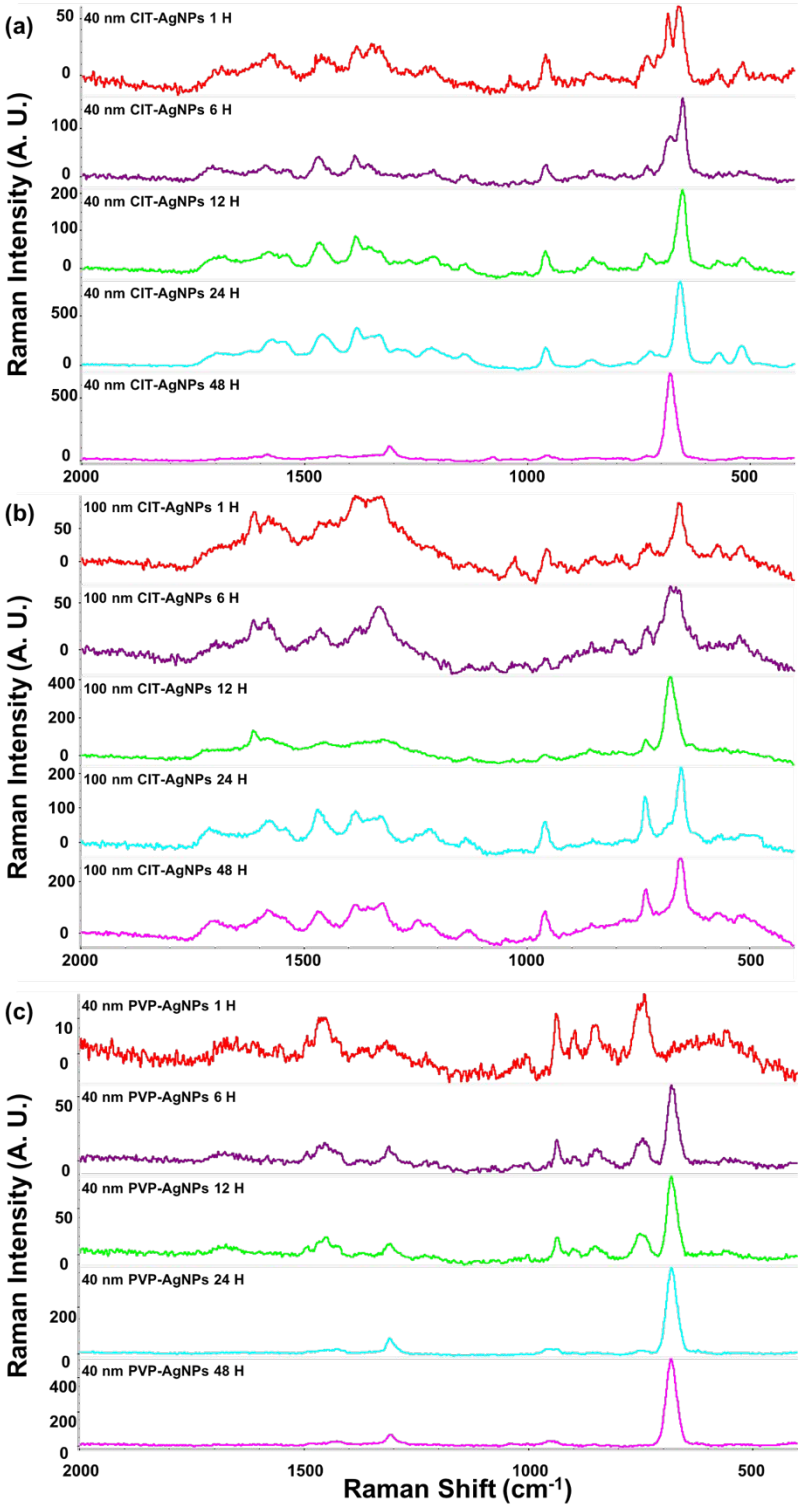
(a)
40 nm CIT-AgNPs 1 H
40 nm CIT-AgNPs 6 H
40 nm CIT-AgNPs 12 H
40 nm CIT-AgNPs 24 H
40 nm CIT-AgNPs 48 H
(b)
100 nm CIT-AgNPs 1 H
100 nm CIT-AgNPs 6 H
100 nm CIT-AgNPs 12 H
100 nm CIT-AgNPs 24 H
100 nm CIT-AgNPs 48 H
(c)
40 nm PVP-AgNPs 1 H
40 nm PVP-AgNPs 6 H
40 nm PVP-AgNPs 12 H
40 nm PVP-AgNPs 24 H
40 nm PVP-AgNPs 48 H
Raman Intensity (A. U.)
Raman Shift (cm-1)
2000
1500
1000
500

Figure 3. *In situ* SERS spectra (Depth: 0 μm) of 40 nm CIT-AgNPs (a), 100 nm CIT-AgNPs (b), 40 nm PVP-AgNPs (c) in spinach following different exposure time.

In addition to particle size, the surface coating is another important factor we investigated in this study. Figure 3c is the *in-situ* SERS spectrum of 40 nm PVP-AgNPs in spinach after different exposure time. Different from the SERS spectra of 40 nm CIT-AgNPs, no distinct peak at 681 cm^{-1} was observed at 1 h for PVP-AgNPs, indicating no immediate interaction between 40 nm PVP-AgNPs and cysteine within such a short time. This observation could be explained by the fact that the molecular weight of PVP is much larger than that of CIT, which would compromise the contact between cysteine and silver atoms at AgNPs surface. After 6 h, the SERS peak at 683 cm^{-1} gradually appeared and became stronger with increasing time, which suggests the replacement of original surface surfactant (PVP) begins. Similarly, we also observed that the SERS intensity of this peak became stronger with time increasing, which indicates more cysteine were produced and further interacted with PVP-AgNPs.

Figure 4c and 4e show the penetration depth profile of 40 nm PVP-AgNPs in spinach. We found the penetration depth of 40 nm PVP-AgNPs increases with increasing foliar exposure time and could reach to 226 ± 47 μm after 48 h ($P > 0.05$). The penetration depth of 40 nm PVP-AgNPs is not statistically different from the penetration depth of 40 nm CIT-AgNPs. This result indicates that surface coating is not a critical factor that determines the penetration ability of AgNPs in spinach. However, it should be noted that 40 nm PVP-AgNPs show lower SERS intensity than 40 nm CIT-AgNPs at the same depth during the first 6 h. We suppose this is because the SERS image was constructed based on the highest C-S stretching and no enhanced C-S stretching peak appeared after 1 h foliar exposure. To further evaluate this, we removed those surface attached AgNPs on spinach and quantified the amounts of residual silver by ICP-MS. As shown in Figure S3, the amounts of residual silver in spinach after 1 and 48 h are non-statistically different, which indicates the PVP-AgNPs also penetrated within the first hours despite the PVP coating was still on the surface.

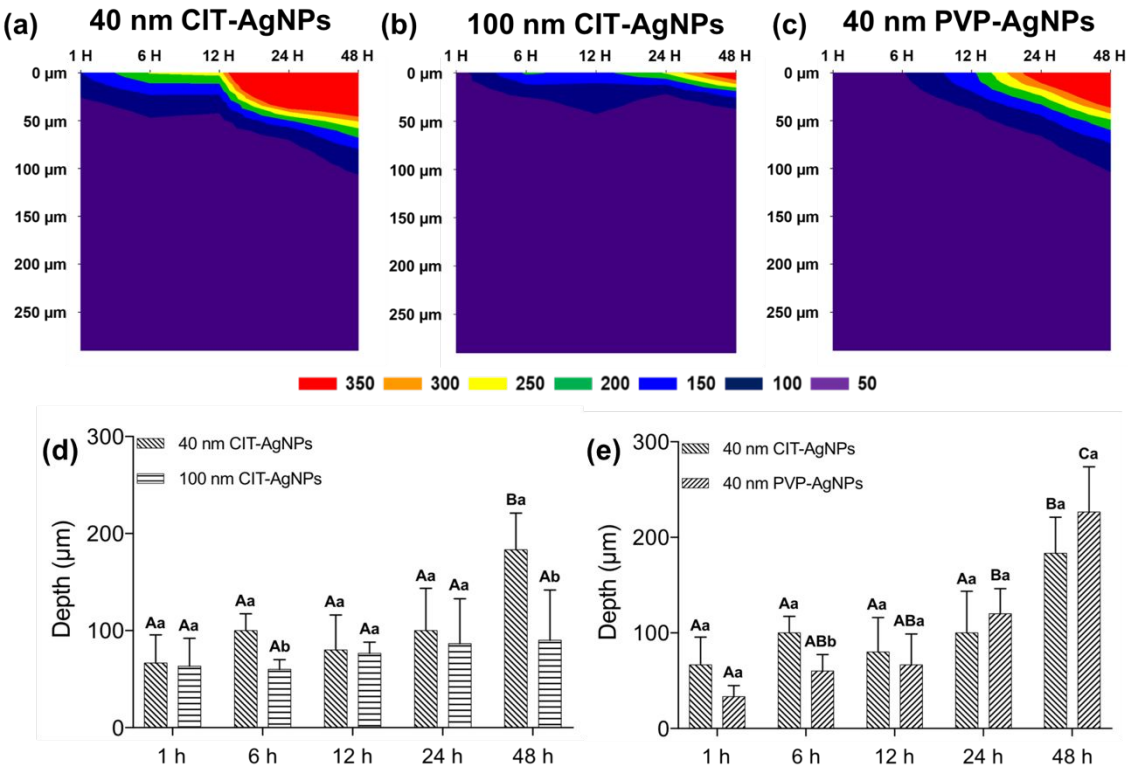

311

312 **Figure 4. SERS depth profiles of (a) 40 nm CIT-AgNPs, (b) 100 nm CIT-AgNPs, (c)**
313 **40 nm PVP-AgNPs penetration following different exposure time based on the highest**
314 **C-S stretching peaks; (d), (e) Comparison of penetration depth of AgNPs with**
315 **different sizes (40 and 100 nm) and surface coatings (CIT and PVP) in spinach**
316 **following different exposure time. Results are expressed as mean value standard**
317 **deviation (n=3). Different capital letters represent a significant difference (P<0.05) of**
318 **the penetration depth of each AgNPs at different foliar exposure time. Different**
319 **lowercase letters mean significant differences (p<0.05) of the penetration depth**
320 **between AgNPs types at the same foliar exposure time.**

321

322 **3.4 Quantification of Penetrated AgNPs in Spinach Leaves.** To determine the amounts
323 of internalized AgNPs in spinach leaves, the first step is to remove those surface attached
324 AgNPs. This is a critical step since incomplete removal may result in overestimation of
325 penetrated AgNPs in spinach leaves. Thus, a combined washing method that using Clorox
326 bleach and ammonium hydroxide was used to clean the spinach leaves and remove those
327 surface attached AgNPs.[6] According to our previous study, this newly developed washing
328 method could effectively remove 91-93% of surface attached AgNPs, which is the most
329 efficient AgNPs removal method so far. After the washing treatment, those penetrated
330 AgNPs in the spinach leaves were extracted by the organic solvent-based method (~50%
331 recovery), which is a novel extraction method developed by our group recently.[14] It is

noteworthy to mention that the morphology of AgNPs would be greatly preserved by this method, which shows its advantage over traditional alkaline/enzymatic extraction method. As shown in Figure 5, we detected hot spots (other than background blue) on the SERS images of 40 nm CIT-AgNPs, 40 nm PVP-AgNPs and 100 nm CIT-AgNPs, respectively. These hot spots are identified as AgNPs based on the intensity threshold (1000 cps) we set, indicating the presence of AgNPs collected on the filter membrane. Based on the number of hot spots (Figure 5), there is no significant difference between 40 nm CIT-AgNPs and 40 nm PVP-AgNPs. However, significantly higher number of hot spots were detected in the images from 40 nm AgNPs than that from 100 nm AgNPs. In addition, in both of the 40 nm AgNPs, higher intensity (red color, indicating strong aggregation) hot spots were detected, as compared to the lower intensity (green color, indicating less aggregation) ones in 100 nm AgNPs. This result indicates there were higher numbers of 40 mm AgNPs than 100 nm ones internalized in the plant tissues after 1 h exposure. To roughly estimate the amounts of internal AgNPs from spinach leaves, we applied previously established standard curves built upon 60 nm AgNPs to quantify the amount of AgNPs based on the percentage of hot spots area in each SERS map. This is because the number of pixels is independent of the peak intensity as long as the intensity is above the cut-off line, indicating this method may be applied to roughly estimate the different sizes or aggregation states of AgNPs. Based on the calculation, the amount we estimated for internal 40 nm AgNPs was 15.5 ± 2.9 ng, which are significantly higher than the amount for internal 100 nm AgNPs, 2.8 ± 2.3 ng. Translating to the %, we estimated around 0.8 ± 0.1% of foliarly applied 40 nm CIT-/PVP-AgNPs and 0.2 ± 0.1% of 100 nm CIT-AgNPs were internalized in the leaf tissues after 1 h exposure. Compared with the total Ag (9-12%) quantified by ICP-MS after washing, the percentage of internal AgNPs quantified by SERS are significantly smaller, which indicates the transformation of AgNPs to SERS inactive Ag-species in spinach leaves. Similar results have also been reported by other groups. For example, Li et al. reported the AgNPs in the leaves after foliar exposure would transform into AgCl-NPs in their recent study. Larue et al. also detected the presence of metallic AgNPs, Ag-glutathione, and other Ag^+ species (predominantly AgCl) in lettuce leaves after foliar exposure.

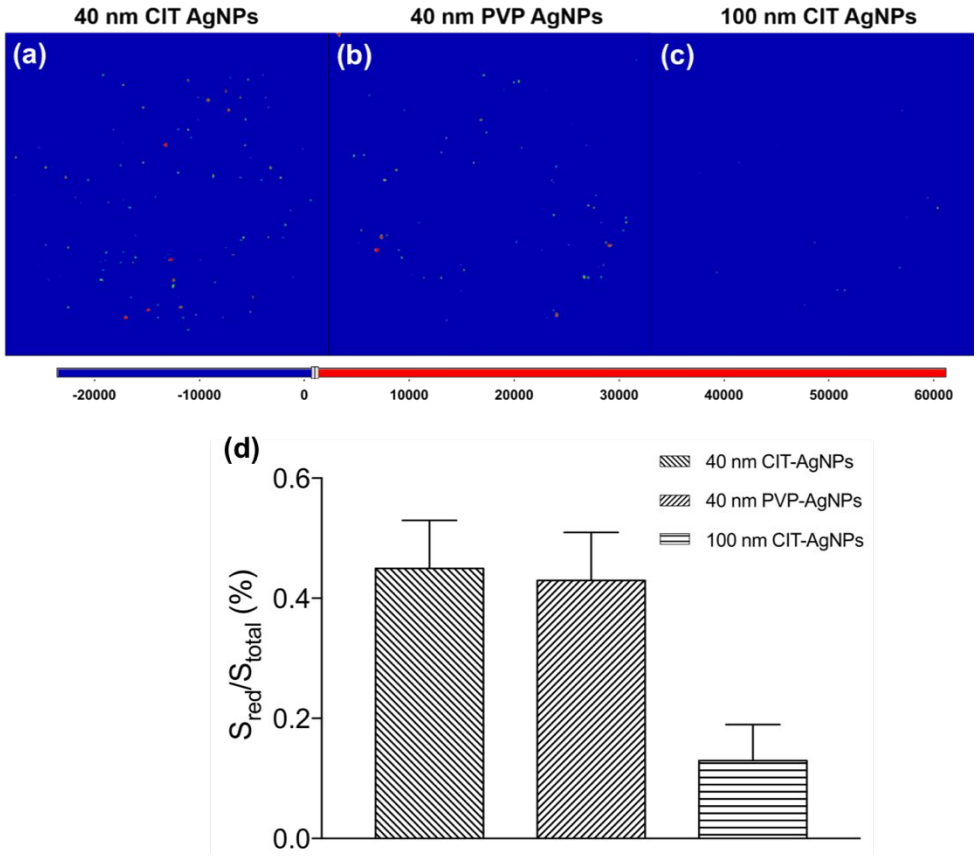

Figure 5. Representative 2D SERS mapping images of filter membranes that were loaded on (A) 40 nm CIT-AgNPs, (B) 40 nm PVP-AgNPs, (C) 100 nm CIT-AgNPs extracted from spinach leaves after 1h.

4. CONCLUSION

Herein, we analyzed the behaviors and biological fate of different kinds of AgNPs in a spinach after different foliar exposure time (1~48 h) using SERS mapping. Results showed that no matter what kind of sizes (40 and 100 nm) and surface coatings (CIT and PVP), all the AgNPs would interact with cysteine and end up with AgNPs-cysteine complex, likely resulted from a detoxification process in plant. In addition, the penetration capability of AgNPs depends on NP size rather than surface coating. After 48 h foliar application, significantly deeper penetration depth and higher amounts of 40 nm CIT-/PVP-AgNPs were detected inside of the leaves as compared to those of the 100 nm CIT-AgNPs. The percentage of internalized AgNPs after 1 hour exposure was in the range of 0.2~0.8%. In addition, ICP-MS results indicate the transformation of AgNPs to other Ag species could occur within 1 hour. Overall, our work gives new insight of behaviors and

biological fate of different kinds of AgNPs in leaves after foliar exposure which will facilitate risk assessment or developing novel pesticide formulations based on AgNPs. Future studies will focus on investigating the behavior and biological fate of AgNPs over a longer exposure time.

ASSOCIATED CONCENT

Supporting information

The supporting information is available free of charge on the publication website.

AUTHOR INFORMATION

Corresponding Author

* E-mail: lilihe@foodsci.umass.edu; Tel: +1 413 545 5847.

Notes

The authors declare no competing financial interest.

ACKNOWLEDGE

We acknowledge USDA-NIFA (2015-67017-23070) for supporting this work.

REFERENCE

1 B. Nowack, H. F. Krug and M. Height, *Environ. Sci. Technol.*, 2011, **45**, 1177–1183.

2 A. A. A S and T. S, *J. Basic Appl. Zool.*, , DOI:10.1186/s41936-019-0124-0.

3 S. W. P. Wijnhoven, W. J. G. M. Peijnenburg, C. A. Herberts, W. I. Hagens, A. G. Oomen, E. H. W. Heugens, B. Roszek, J. Bisschops, I. Gosens and D. Van De Meent, *Nanotoxicology*, 2009, **3**, 109–138.

4 E. Schreck, Y. Foucault, G. Sarret, S. Sobanska, L. Cécillon, M. Castrec-Rouelle, G. Uzu and C. Dumat, *Sci. Total Environ.*, 2012, **427**, 253–262.

5 E. McGillicuddy, I. Murray, S. Kavanagh, L. Morrison, A. Fogarty, M. Cormican, P. Dockery, M. Prendergast, N. Rowan and D. Morris, *Sci. Total Environ.*, 2017, **575**, 231–246.

6 Z. Zhang, H. Guo, C. Ma, M. Xia, J. C. White, B. Xing and L. He, *Food Control*, 2018, **In Press,** https://doi.org/10.1016/j.foodcont.2018.11.005.

7 A. Noori, A. Ngo, P. Gutierrez, S. Theberge and J. C. White, *J. Nanoparticle Res.*, , DOI:10.1007/s11051-020-04866-y.

8 J. P. Stegemeier, B. P. Colman, F. Schwab, M. R. Wiesner and G. V. Lowry, *Environ. Sci. Technol.*, 2017, **51**, 4936–4943.

9 C. O. Dimkpa, J. E. McLean, N. Martineau, D. W. Britt, R. Haverkamp and A. J. Anderson, *Environ. Sci. Technol.*, 2013, **47**, 1082–1090.

10 C. Larue, H. Castillo-Michel, S. Sobanska, L. Cécillon, S. Bureau, V. Barthès, L. Ouerdane, M. Carrière and G. Sarret, *J. Hazard. Mater.*, 2014, **264**, 98–106.

11 Z. Zhang, H. Guo, Y. Deng, B. Xing and L. He, *RSC Adv.*, 2016, **6**, 1–

22.

12 R. Lahr and P. Vikesland, *ACS Sustain. Chem. ...*, 2014, A-J.

13 a G. Shen, J. Z. Guo, W. Xie, M. X. Sun, R. Richards and J. M. Hu, *J. Raman Spectrosc.*, 2011, **42**, 879–884.

14 Z. Zhang, M. Xia, C. Ma, H. Guo, W. Wu, J. White, B. Xing and L. He, *Environ. Sci. Nano*, , DOI:10.1039/c9en01246j.

15 T. M. Tolaymat, A. M. El Badawy, A. Genaidy, K. G. Scheckel, T. P. Luxton and M. Suidan, *Sci. Total Environ.*, 2010, **408**, 999–1006.

16 Z. Zhang, H. Guo, T. Carlisle, A. Mukherjee, A. Kinchla, J. C. White, B. Xing and L. He, *J. Agric. Food Chem.*, 2016, acs.jafc.6b02705.

17 R. Salemmilani, R. Y. Mirsafavi, A. W. Fountain, M. Moskovits and C. D. Meinhart, *Analyst*, 2019, **144**, 1818–1824.

18 R. Raliya, C. Franke, S. Chavalmane, R. Nair, N. Reed and P. Biswas, *Front. Plant Sci.*, 2016, **7**, 1–10.

19 P. S. Ghosh, C. K. Kim, G. Han, N. S. Forbes and V. M. Rotello, *ACS Nano*, 2008, **2**, 2213–2218.

20 A. S. Thakor, J. Jokerst, C. Zavaleta, T. F. Massoud and S. S. Gambhir, *Nano Lett.*, 2011, **11**, 4029–4036.

21 C. Ma, S. Chhikara, R. Minocha, S. Long, C. Musante, J. C. White, B. Xing and O. P. Dhankher, *Environ. Sci. Technol.*, 2015, **49**, 10117–

10126.

22 C. C. Li, F. Dang, M. Li, M. Zhu, H. Zhong, H. Hintelmann and D. M. Zhou, *Nanotoxicology*, 2017, **11**, 699–709.

23 C. Cobbett and P. Goldsbrough, *Annu. Rev. Plant Biol.*, 2002, **53**, 159–182.

24 G. D. Fleming, J. J. Finnerty, M. Campos-Vallette, F. Celis, A. E. Aliaga, C. Fredes and R. Koch, *J. Raman Spectrosc.*, 2009, **40**, 632–638.

25 C. Jing and Y. Fang, *Chem. Phys.*, 2007, **332**, 27–32.

26 J. D. Judy, J. M. Unrine, W. Rao, S. Wirick and P. M. Bertsch, *Environ. Sci. Technol.*, 2012, **46**, 8467–8474.

27 M. Espina Palanco, K. B. Mogensen and K. Kneipp, *J. Raman Spectrosc.*, 2016, **47**, 156–161.

28 Y. Li, O. P. Dankher, L. Carreira, A. P. Smith and R. B. Meagher, *Plant Physiol.*, 2006, **141**, 288–298.

29 T. Eichert, A. Kurtz, U. Steiner and H. E. Goldbach, *Physiol. Plant.*, 2008, **134**, 151–160.

30 W.-N. Wang, J. C. Tarafdar and P. Biswas, *J. nanoparticle Res.*, 2013, **15**, 1–13.

SUPPORTING INFORMATION

In situ and Real Time Investigation of Foliarly Applied Silver Nanoparticles in Spinach Leaves by Surface Enhanced Raman Spectroscopic Mapping Technique

Zhiyun Zhang[1], Heping Shang[2], Baoshan Xing[2], and Lili He[1]

[1]Department of Food Science, University of Massachusetts, Amherst, Massachusetts 01003, United States

[2]Stockbridge School of Agriculture, University of Massachusetts, Amherst, Massachusetts 01003, United States

*** Corresponding Author:** Lili He,

Mailing Address: 240 Chenoweth Laboratory, 102 Holdsworth Way, Amherst, MA 01003,

E-mail: lilihe@foodsci.umass.edu,

Telephone: +1 (413) 545-5847

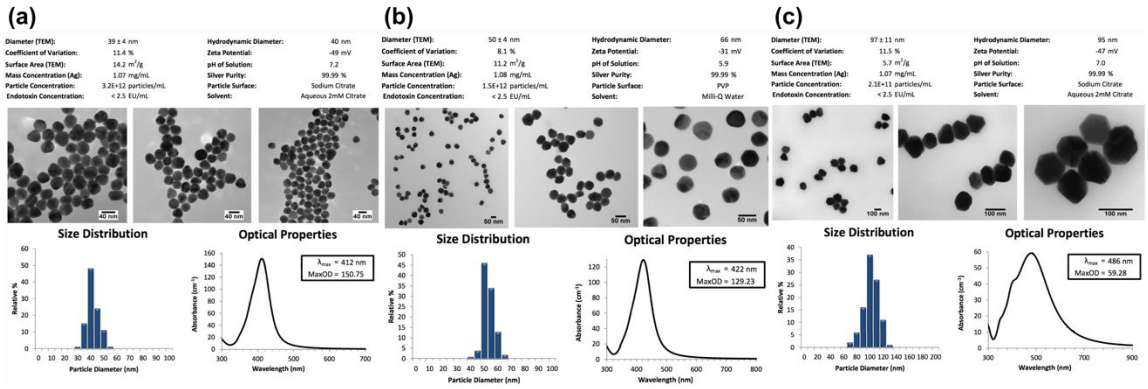

Figure S1. The basic information of used AgNPs from nanocomposix.

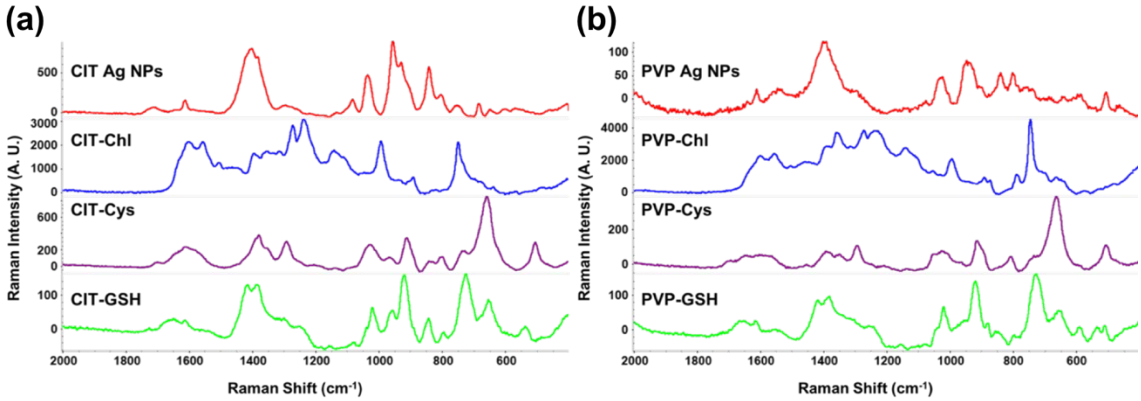

Figure S2. In vitro SERS spectra of chlorophyll, cysteine, and glutathione.

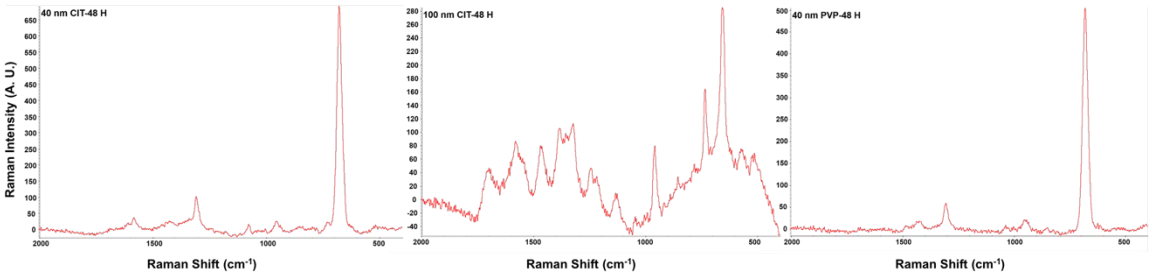

Figure S3. ***In situ*** **SERS spectra (Depth: 0 μm) of 40 nm CIT-AgNPs (a), 100 nm CIT-AgNPs (b), 40 nm PVP-AgNPs (c) in spinach after 48 h.**

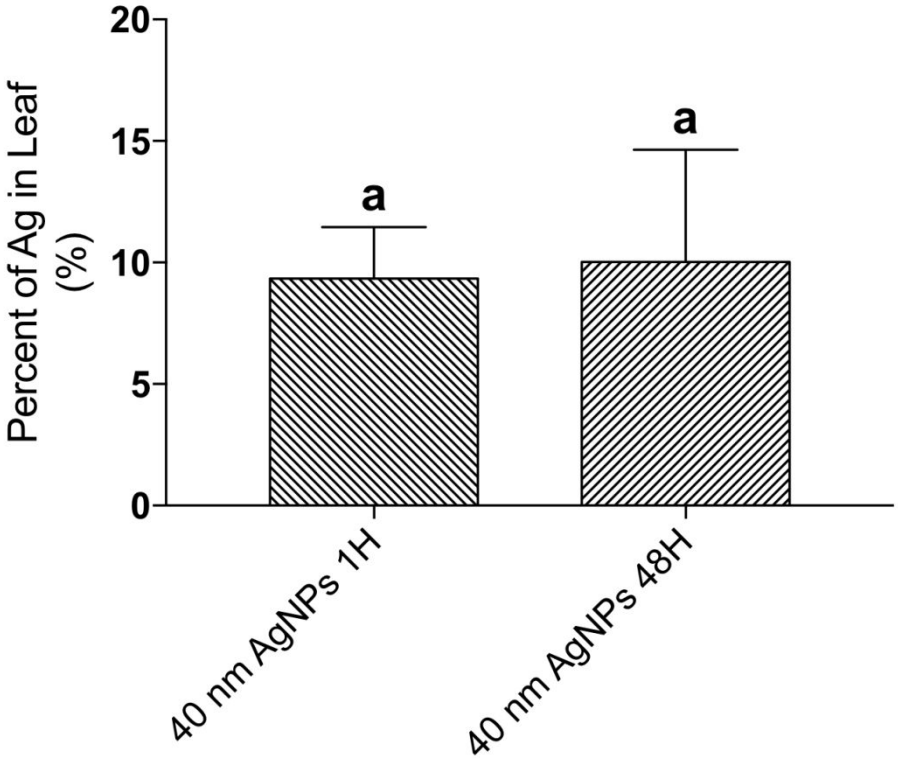

Figure S4. The amounts of penetrated Ag in spinach leaves by ICP-MS. Same letter represents a non-statistically significant difference (P>0.05).

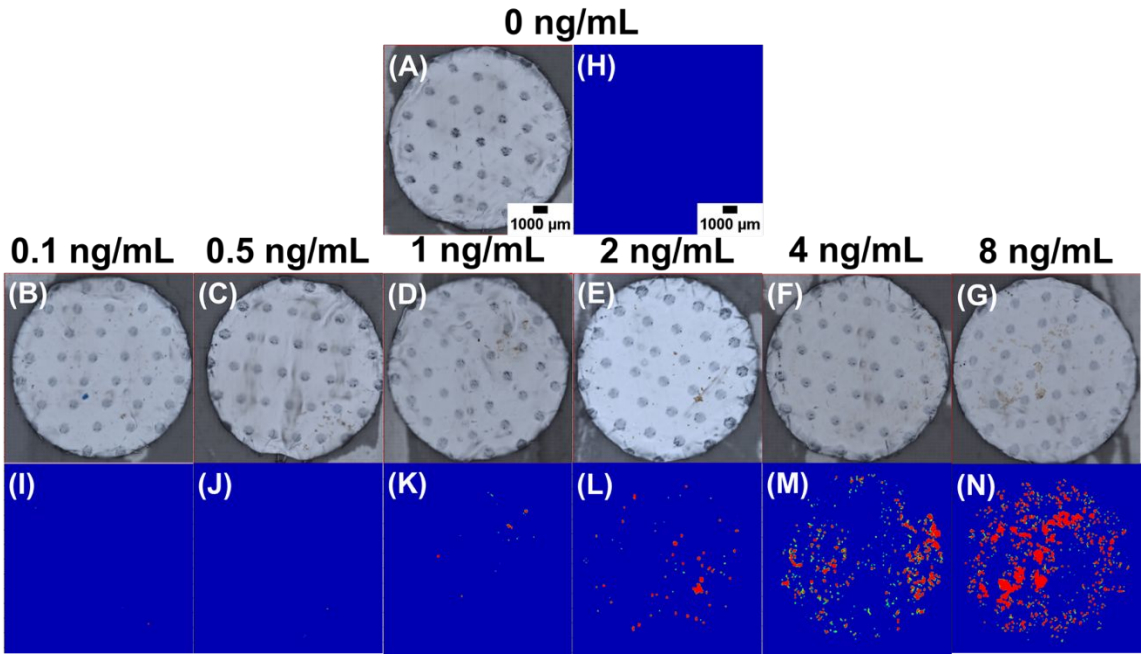

Fig. S5 Different amount of 60 nm CIT-AgNPs on the filter membrane. Optical images: (A)-(C), (G)-(I); Raman scattering images: (D)-(F), (J)-(L). Laser wavelength=780 nm, Laser intensity=5 mW, aperture= 50 slit, step size= 100 µm, scan rate=0.05 s/step.[14]